Available online at www.sciencedirect.com

ScienceDirect

Procedia Engineering 98 (2014) 71 – 77

Procedia Engineering

www.elsevier.com/locate/procedia

11th International Symposium on Systems with Fast Ionic Transport, ISSFIT 11

Phase separation and electrical properties of manganese borosilicate glasses

Piotr Kupracz*, Natalia Anna Szreder, Maria Gazda, Jakub Karczewski, Ryszard Jan Barczyński

Faculty of Applied Physics and Mathematics, Gdańsk University of Technology, ul. Narutowicza 11/12, 80-233 Gdańsk, Poland

Abstract

The structure and electrical properties of manganese borosilicate glasses of a composition of $xMnO\text{-}(0.8\text{-}x)SiO_2\text{-}(0.2)B_2O_3$ (x=0.4, 0.5 and 0.6 in mol) were investigated by impedance spectroscopy, SEM, XRD and confocal microscopy methods. The influence of composition on the glass structure and electrical properties was discussed. A separation of two amorphous phases was observed and it was concluded that one phase is SiO_2-rich and the other is MnO-rich. It was found that the direct current conductivity and the activation energy of conductivity decreases with an increase in the manganese oxide content. The proposed mechanism of the conductivity is overlapping large polaron hopping.

Peer-review under responsibility of the Gdansk University of Technology

Keywords: impedance spectroscopy; borosilicate glass; manganese oxide; conductivity;

1. Introduction

Many authors studied manganese borate, borosilicate and manganese borosilicate glasses with regard to the effect of the glass composition on its structural properties [1-6]. The NMR studies [2] revealed that in $xB_2O_3\text{-}(1\text{-}x)SiO_2$ glass, B_2O_3 can be incorporated into the SiO_2 matrix without a phase separation up to a limit of x=0.5 (in mol). Similar effect was observed in $xB_2O_3\text{-}(1\text{-}x)MnO$ glass, in which the phase separation occurred when x exceeds 0.5 [3]. In low alkaline borosilicate glasses phase separation depends on alkaline oxides content. For instance, in Duran glass ($83SiO_2\text{-}12B_2O_3\text{-}4Na_2O\text{-}1Al_2O_3$ in mol%) phase separation occurred when MnO content exceeded 4mol% [1].

* Corresponding author. Tel.: +48-583-486-604;
E-mail address: pkupracz@mif.pg.gda.pl

Peer-review under responsibility of the Gdansk University of Technology
doi:10.1016/j.proeng.2014.12.490

There are reports that the electron paramagnetic resonance, the infrared spectroscopy and high energy X-ray absorption near edge structure (XANES) were used for probing atomic coordination and clusters formation in MnO-B_2O_3 glasses [4-6]. Kajinami et al. [4] showed that the mean distance of B-O linkage and the coordination number of boron increases with increasing MnO content. Clustering of octahedral MnO_6 units was shown by Winterstein-Beckmann et al. [5] in glass with a composition of (1–2x)MnO-x(SrO-B_2O_3) until x does not exceed 0.46. Rumori et al. [6] suggested that manganese could be inserted homogeneously into the glassy matrix of borosilicate or silicate glasses only when alkaline ions are present. In other conditions, manganese appear as separated MnO-rich microphases.

Many work was done to determine parameters and models of conductivity in glasses containing manganese oxide. Dutta et al. performed measurements on phosphorous glasses containing manganese and iron [7] or vanadium [8] oxides. They showed that a transport mechanism of conductivity is the hoping of small polarons between multivalent vanadium or iron ions and the Mn ions do not appear to have any direct contribution to the conductivity of these glasses. Measurements made by Annamlai et al. [9] on glass system Fe_2O_3-MnO-TeO_2 confirm the transport mechanism as small polaron hopping and they show that the hopping occurs between both manganese and iron ions. So far, no measurements of conductivity on glass system MnO-SiO_2-B_2O_3 were performed.

The aim of the presented study is to compare the microstructure and electrical properties of manganese borosilicate glasses.

2. Experimental

Samples with a nominal composition of xMnO-(0.8-x)SiO_2-(0.2)B_2O_3 where x=0.4, 0.5 and 0.6 (molar ratio) were prepared. An appropriate amounts of analytical grade powders of MnO (Sigma-Aldrich), SiO_2 (POCH) and H_3BO_3 (POCH) were milled in an agate mortar. The obtained powders were melted in air at the temperature of 1470K, 1370K and 1670K for x=0.6, 0.5 and 0.4 respectively for 30 minutes. Melts were quenched between two preheated to temperature about 600K metal plates to obtain round pellets (1-2mm thick and 10-20mm in diameter).

The differential scanning calorimetry (DSC) measurements were performed to determine the glass transition temperature. The thermal analysis was done on 40mg of powder samples in current nitrogen flow of 50cm^3min^{-1} using thermal analyzer Netzsch STA 449F1. The heating rate was maintained at 15$Kmin^{-1}$ in the temperature range from 370K to 1170K.

The microstructure of the samples was investigated with scanning electron microscope FEI Company Quanta FEG250 and confocal microscope Olympus OLS 4000 Lext with a CCD camera. The XRD spectra were studied by the X-ray diffraction method with Philips X'Pert Pro MPD using CuKα radiation.

Impedance spectroscopy measurements were carried out in the temperature range of 370K–720K (below glass transition temperature) with Novocontrol Concept 40 broadband dielectric spectrometer and high temperature

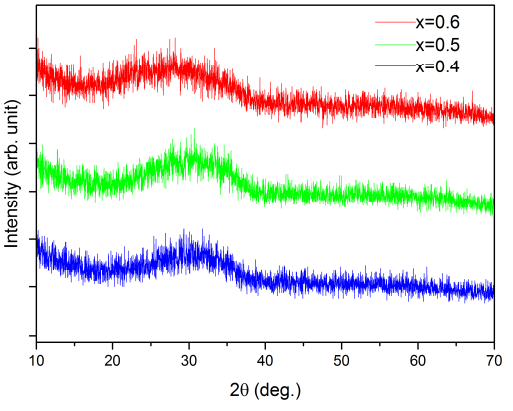

Fig. 1. The XRD patterns obtained for all samples.

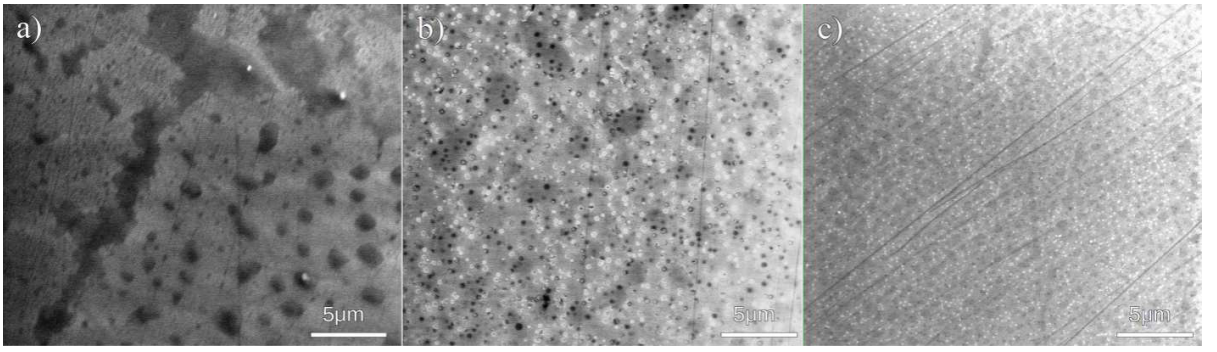

Fig. 2. SEM images of polished cross section of obtained glasses for a)x=0.4, b)x=0.5 and c)x=0.6.

controller Novotherm-HT 1600. The frequency range was from 10mHz to 1MHz and the ac signal was $1V_{rms}$. Gold electrodes were prepared by sputtering in vacuum.

3. Results and Discussion

The XRD patterns of obtained samples are shown in Fig. 1. For all systems, the diagram is typical of the amorphous material.

Figure 2 presents SEM images of polished cross sections of the pellets. It could be seen that in each sample a separation of two phases occurs. In material with x=0.5 and x=0.6 (Fig. 2b and 2c) uniformly dispersed brighter granules are visible as circular areas in darker background. These granules have a diameter of about 400nm and 200nm for samples with x=0.5 and x=0.6 respectively. In the sample with x=0.4 (Fig. 2a) the dispersed areas are darker than the background and their shapes is irregular. Some of them have a diameter of about 100nm while others of about 1000nm. There are also regions where phase seen as darker create a continuous path of length more than 30µm.

Ehrt [3] showed that the melts of ternary systems $MnO\text{-}SiO_2\text{-}B_2O_3$ and $ZnO\text{-}SiO_2\text{-}B_2O_3$ separate into SiO_2 rich and zinc or manganese rich phase and revealed that the addition of Na_2O decrease phase separation.

A comparison of all obtained SEM pictures (Fig. 2) shows that a volume ratio of the phase seen as bright decreases with a decrease in silicon oxide content. This observation could indicate that one of the existing phases, seen as light in SEM images, is SiO_2-rich while the other is $MnO\text{-}B_2O_3$-rich. A microstructure of glasses suggests that a point when a volume ratio between observed phases is equal to one lays in the range of $0.4 \leq x \leq 0.5$.

The determined glass transition temperature is listed in Tab. 1. The temperature of transition is 843K, 828K and 826K (±7K) for the sample with x equal to 0.4, 0.5 and 0.6 respectively.

UV-Vis absorption measurements made by Mocke et al. [1], Ehrt [3] and Winterstein-Beckmann et al. [5]

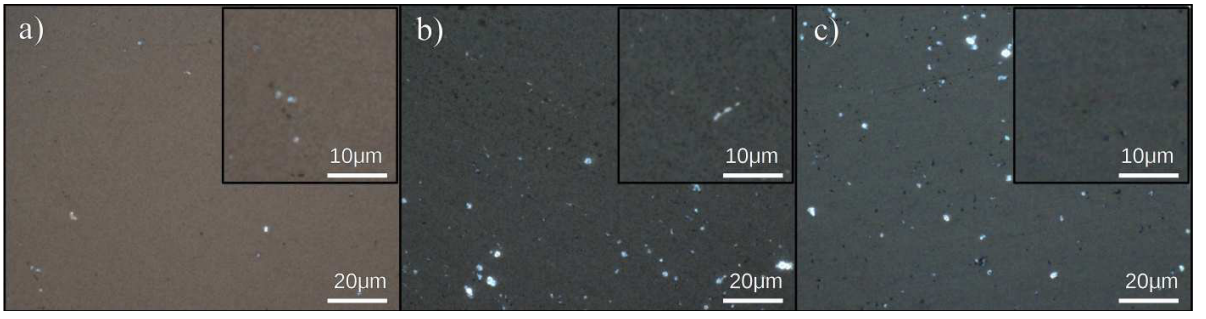

Fig. 3. Confocal microscope images of the cross sections of glass with a composition $xMnO\text{-}(0.8\text{-}x)SiO_2\text{-}(0.2)B_2O_3$: a) x=0.4, b) x=0.5 and c) x=0.6. In the image b) small dark areas of about 0.5µm are present.

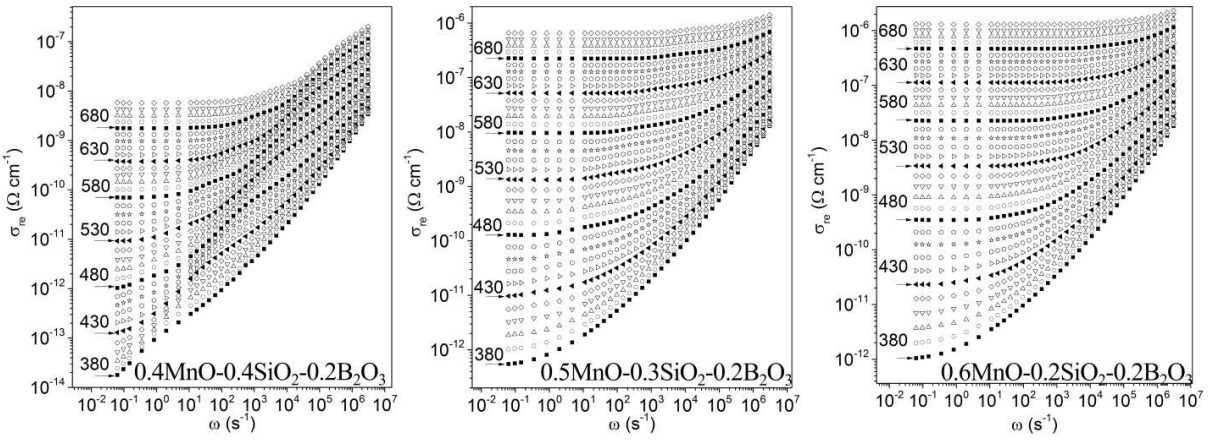

Fig. 4. Graphs of real part of conductivity (σ_{re}) in function of angular frequency in temperature ranges 380K≤T≤720K in step of 10K.

showed that the observed color of glasses containing manganese oxide is mainly correlated with the presence of Mn^{3+} ions. The color of glass become darker with an increase in Mn^{3+} ions concentration. The equilibrium between Mn^{2+} and Mn^{3+} should be shifted toward a higher oxidation state with increase in optical basicity which increases with MnO content [5,10].

Different colors of obtained samples were observed. For x=0.4 the glass was light brown, for x=0.5 dark brown and for x=0.6 whole black. This observation gives information that the concentration of Mn^{3+} ions increases with the amount of MnO.

Images of glasses cross sections made with the confocal microscope are presented in Fig. 3. Before imaging, samples were cut and polished. In images a) and c) it could be seen that the glasses are homogenous and in an image b) representing the sample with x=0.5 small oval structures of about 0.5μm in diameter are visible. A confocal microscopy image of the light brown sample does not show phase separation (Fig. 3a) which is seen in the SEM image (Fig. 2a). It could be explained by small differences in color of existing phases in the glass. Sizes of oval regions presented in SEM and confocal microscopy images of sample with x=0.5 are similar. This observation could indicate that they represent the same SiO_2-rich phase. In the sample with x=0.6, diameters of the SiO_2-rich phase areas measured in SEM images are smaller than a half of visible light wavelength and, in consequence, they are

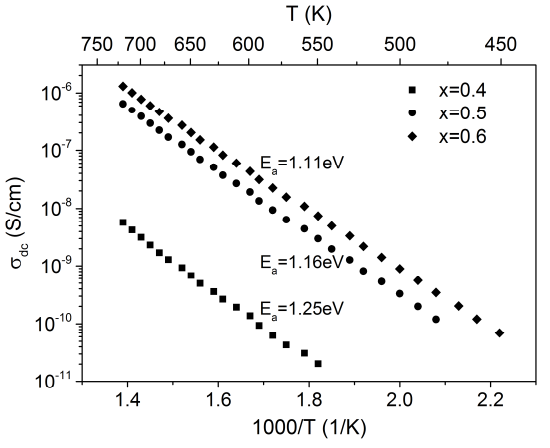

Fig. 5. Chart present real part of conductivity in function of inverted temperature.

below the resolution range of the confocal microscope.

The confocal microscopy results confirm a presence of two separated phases in the dark brown sample. Moreover, dark colors of SiO_2-rich phase presented in this sample could indicate that the concentration of Mn^{3+} ions is higher in that phase than in the MnO-rich matrix phase.

3.2. Electrical properties

Table 1. Properties of glass series including temperature of pouring and glass transition, conductivity at 680K and activation energy found of conductivity.

Composition	T_m (K)	T_g (K)	$\sigma_{DC\ at\ 680K}$ (10^{-7} S/cm)	E_a (eV)
$0.4MnO\text{-}0.4SiO_2\text{-}0.2B_2O_3$	1670	843	1.71×10^{-2}	1.25
$0.5MnO\text{-}0.3SiO_2\text{-}0.2B_2O_3$	1370	828	2.22	1.16
$0.6MnO\text{-}0.2SiO_2\text{-}0.2B_2O_3$	1470	826	4.66	1.11

Figure 4 presents plots of a real part of conductivity (σ_{re}) versus angular frequency in a temperature range of 380K≤T≤720K. The plots consist of three regions: a dc plateau dominating in low frequency region, an ac component increasing in linear fashion with frequency and an intermediate region. In many materials, the relation between conductivity and frequency could be described by the universal dynamic response which was introduce by Jonsher [11] and it is expressed by the equation:

$$\sigma_{re} = \sigma_{dc} + A\omega^{s(T)} \qquad (1)$$

where σ_{dc} is the dc conductivity, A is a constant, ω is an angular frequency and the exponent s is a function of temperature. However, because of presence of additional relaxation processes, the obtained materials does not obey that Eq. 1 in all the examined frequency range. It may be seen that at a temperature of 680K for samples with x=0.5 and x=0.6 (Fig. 4) a contribution to conductivity of this additional relaxation processes is seen on the ac component around $\omega=10^4$ (s^{-1}) and $\omega=10^5$ (s^{-1}) respectively. In the sample with x=0.4 the contribution of two additional relaxation processes is visible at frequency around $\omega=10^4$ (s^{-1}) and $\omega=10^6$ (s^{-1}). In all cases the contribution of additional relaxation processes to real part of conductivity are temperature dependent.

Direct current conductivity (σ_{dc}) was found as a value of the dc plateau and it was plotted versus reciprocal temperature in Fig. 5. The conductivity increases with increasing temperature. The activation energy was calculated from the Arrhenius law given by the relation:

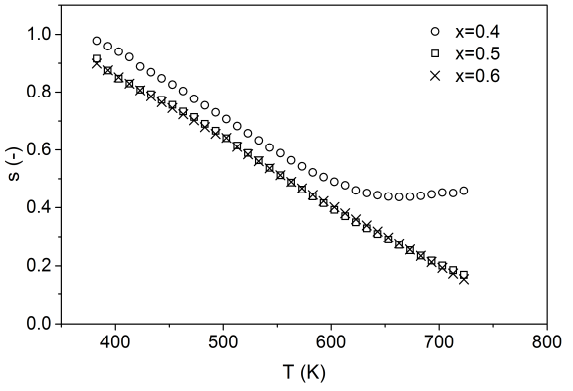

Fig. 6. Image present the plot parameter s versus temperature at $\omega=8.37\times10^5$ s^{-1} versus temperature.

$$\sigma_{dc}T = \sigma_0 + \exp(\frac{-E_a}{kT}) \quad (2)$$

where E_a is the activation energy of conductivity, k is a Boltzmann constant and σ_0 is the pre-exponential factor. The evaluated values of activation energy are1.25±0.06eV, 1.16±0.05eV and 1.11±0.05eV for samples with x=0.4, 0.5 and 0.6 respectively. It can be seen that both parameters decrease with increase in the manganese oxide content. A comparison of microstructure (Fig. 2) and conductivity properties (Tab. 1) shows that the dc conductivity increases with increase in volume ratio of phase seen as dark in SEM images. It indicates that the conductivity of that phase is higher than the conductivity of the other phase. Moreover, when this phase becomes dispersed in the light phase (x changes from 0.5 to 0.4), the conductivity of glass decreases over two orders of magnitude. Changes in conductivity compared with microstructure validate the assumption that the phase seen as darker is MnO-rich.

There are many reports [12-14] that in transition metal oxide glasses mechanism of conductivity called polaron hopping occurs. That model assumed that the charge carrier together with its self-induced polarization cloud (together called polaron) moves between ions in glass matrix [15]. If polarons are so localized that their distortion cloud do not overlap they are called small in the other case they are called large [16]. Analysis of s parameter could be used to choose adequate theory to described model of conductivity in measured glasses. Changes of the s parameter versus temperature described by the small polaron hopping model are represent by Eq. 3a and described by the large polaron hopping model are represent by Eq. 3b [16].

$$s = 1 - \frac{4}{\ln\left(\frac{1}{\omega\tau_0}\right) - \frac{W_H}{kT}} \quad (3a)$$

$$s = 1 - \frac{1}{R_w}\frac{4 + 6\left(\frac{W_H r_0}{kTR_w^2}\right)}{\left(1 + \frac{W_H r_0}{kTR_w^2}\right)^2} \quad (3b)$$

where τ_0 is a relaxation time, W_H is an activation energy of polaron transfer, R_w is a tunneling distance and r_0 is a large polaron radius [16].

In the small polaron hopping model the s parameter increases with temperature (Eq. 3a) while in the large polaron hopping model (Eq. 3b) it should decrease until it reaches a minimum value. The exponent s was evaluated as a derivative of plots represented in Fig. 4. Measured values at the angular frequency $\omega=8.37\times10^5$ s^{-1} are represented as a function of temperature in Fig. 6. As it could be seen, in two samples with x=0.5 and 0.6 the exponent parameter decreases in a linear fashion with temperature. In the sample of a composition of 0.4MnO-0.4SiO_2-0.2B_2O_3 the value of parameter s also decreases linearly to temperature about 600K, then it reaches minimum around 650K and starts to increase slowly. Changes of the s parameter like these represented in Fig. 6 are consistent with large polaron hopping theory (Eq. 3b).

4. Conclusion

A study on manganese borosilicate glasses was reported. The XRD and SEM measurements showed a presence of two amorphous phases: SiO_2-rich and MnO-rich. The confocal microscopy confirms the presence of phase separation in the sample of a composition 0.5MnO-0.3SiO_2-0.2B_2O_3 but it was unable to confirm that phenomenon in a sample with higher manganese oxide content because of the limits of the confocal microscopy resolution. Difference between colors of phases present in the dark brown sample suggests that the SiO_2-rich phase exhibit higher concentration of Mn^{3+} ions than the rest of the sample.

The dc conductivity of the glass with the highest manganese oxide content was determined as two times higher than the conductivity of that with a composition of $0.5MnO\text{-}0.3SiO_2\text{-}0.2B_2O_3$ and over two orders of magnitude higher than the conductivity of the lowest manganese oxide content glass. It was shown that the activation energy of conductivity decreases with an increase in Mn content. On the basis of dependence of the exponent parameter s on temperature, we believe that the overlapping large polaron hopping is the process responsible for conductivity in manganese borosilicate glasses.

References

[1] D. Möncke, E.I. Kamitsos, A. Herrmann, D. Ehrt, M. Friedrich, Bonding and ion–ion interactions of Mn^{2+} ions in fluoride-phosphate and boro-silicate glasses probed by EPR and fluorescence spectroscopy, J. Non-Cryst. Solids 357 (2011) 2542-2551.

[2] L. van Wüllen, G. Schwering, ^{11}B-MQMAS and ^{29}Si-^{11}B Double Resonance NMR Studies on the Structure of Binary B_2O_3-SiO_2 Glasses, Solid State Nuc. Mag. Res. 21 (2002) 134-144.

[3] D. Ehrt, Zinc and manganese borate glasses – phase separation, crystallisation, photoluminescence and structure, Phys. Chem. Glasses: Eur. J. Glass Sci. Technol. B 54 (2013) 65-75.

[4] A. Kajinami, T. Kotake, S. Deki, S. Kohara, The structural analysis of manganese borate glass by high-energy X-ray diffraction measurement, Nucl. Instr. Meth. B 199 (2003) 34–37.

[5] A. Winterstein-Beckmann, D. Möncke, D. Palles, E.I. Kamitsos, L. Wondraczek, Structure property in highly modified Sr, Mn-borate glasses, J. Non-Cryst. Solids 376 (2013) 165-174.

[6] P. Rumori, B. Deroide, N. Abidi, H. El Mkami, J.V. Zanchetta, Mn^{2+} electron paramagnetic resonance study of a sodium borosilicate glass prepared by the sol-gel method, J. Phys. Chem. Solids 59 (1998) 959-967.

[7] B. Dutta, N. A. Fahmy, I. L. Pegg, Effect of mixed transition-metal ions in glasses. Part III: The P_2O_5–V_2O_5–MnO system, J. Non-Cryst. Solids 352 (2006) 2100–2108.

[8] B. Dutta, N. A. Fahmy, and I. L. Pegg, Effect of mixing transition ions in glasses. II. The P_2O_5–Fe_2O_3–MnO system, J. Non-Cryst. Solids 351 (2005) 2552–2561.

[9] S. Annamalai, R. P. Bhatta, I. L. Pegg, and B. Dutta, Mixed transition-ion effect in the glass system: Fe_2O_3-MnO-TeO_2, J. Non-Cryst. Solids 358 (2112) 1380–1386.

[10] J. A. Duffy, A review of optical basicity and its applications to oxidic systems, Geochim. Cosmochim. Acta 57 (1993) 3961–3970.

[11] A.K. Jonscher, Dielectric relaxation in solids, Chelsea Dielectric Press, London, 1983.

[12] S.R. Elliott, A.c. conduction in amorphous chalcogenide and pnictide semiconductors, Adv. in Phys. 36 (1986) 135-218.

[13] L. Murawski, A.c conductivity in binary V_2O_5-P_2O_5 glasses, Phil. Mag. B 50 (1984) L69-L74.

[14] L. Murawski, R.J. Barczyński, Electronic and ionic relaxations in oxide glasses, Solid State Ionics 176 (2005) 2145-2151.

[15] N.F. Mott, Conduction in glasses containing transition metal ions, J. Non-Cryst. Solids 1 (1968) 1-17.

[16] T. Holstein, Studies of polaron motion: Part I. The molecular-crystal model, Ann. Phys. 8 (1959) 325-342.